Simultaneous optimization of dose distributions and fractionation schemes in particle radiotherapy

Jan Unkelbach[a] and Chuan Zeng
Department of Radiation Oncology, Massachusetts General Hospital and Harvard Medical School, Boston, Massachusetts 02114

Martijn Engelsman
Faculty of Applied Physics, Delft University of Technology/HollandPTC, 2628 CJ Delft, The Netherlands

(Received 4 April 2013; revised 19 June 2013; accepted for publication 11 July 2013; published 5 August 2013)

Purpose: The paper considers the fractionation problem in intensity modulated proton therapy (IMPT). Conventionally, IMPT fields are optimized independently of the fractionation scheme. In this work, we discuss the simultaneous optimization of fractionation scheme and pencil beam intensities.
Methods: This is performed by allowing for distinct pencil beam intensities in each fraction, which are optimized using objective and constraint functions based on biologically equivalent dose (BED). The paper presents a model that mimics an IMPT treatment with a single incident beam direction for which the optimal fractionation scheme can be determined despite the nonconvexity of the BED-based treatment planning problem.
Results: For this model, it is shown that a small α/β ratio in the tumor gives rise to a hypofractionated treatment, whereas a large α/β ratio gives rise to hyperfractionation. It is further demonstrated that, for intermediate α/β ratios in the tumor, a nonuniform fractionation scheme emerges, in which it is optimal to deliver different dose distributions in subsequent fractions. The intuitive explanation for this phenomenon is as follows: By varying the dose distribution in the tumor between fractions, the same total BED can be achieved with a lower physical dose. If it is possible to achieve this dose variation in the tumor without varying the dose in the normal tissue (which would have an adverse effect), the reduction in physical dose may lead to a net reduction of the normal tissue BED. For proton therapy, this is indeed possible to some degree because the entrance dose is mostly independent of the range of the proton pencil beam.
Conclusions: The paper provides conceptual insight into the interdependence of optimal fractionation schemes and the spatial optimization of dose distributions. It demonstrates the emergence of nonuniform fractionation schemes that arise from the standard BED model when IMPT fields and fractionation scheme are optimized simultaneously. Although the projected benefits are likely to be small, the approach may give rise to an improved therapeutic ratio for tumors treated with stereotactic techniques to high doses per fraction. [http://dx.doi.org/10.1118/1.4816658]

Key words: proton therapy optimization, non-uniform fractionation, biologically equivalent dose

1. INTRODUCTION

In current clinical practice, most radiotherapy treatments are fractionated. This approach is motivated by the observation that most healthy tissues, compared to most tumors, have a greater ability to recover from radiation damage in between fractions.[1] In most cases, the patient is treated with the same dose distribution over the entire treatment course. Furthermore, the physically achievable dose distribution and the fractionation schedule (i.e., the number of fractions) are determined sequentially.[2]

In intensity-modulated radiotherapy with photons (IMRT) or protons (IMPT), the dose distribution delivered to the patient is determined by solving a *fluence map optimization* problem. This is performed using mathematical optimization techniques that minimize a dose-based objective function with respect to the intensity of individual beam segments. In a typical scenario, treatment plan optimization aims at delivering the prescribed dose to the tumor, while sparing adjacent healthy tissues as much as possible.

The fractionation scheme is driven by the outcome of clinical trails comparing different fractionation schemes. The most common approach to relate and compare dose prescriptions for different fractionation schemes is based on the concept of biologically equivalent dose (BED).[3] For a treatment with a uniform fractionation scheme, i.e., in each of n fractions, the dose d is delivered to a volume of interest, the BED is given by

$$\mathrm{b} = nd\left(1 + \frac{d}{(\alpha/\beta)}\right), \tag{1}$$

where the α/β-ratio is the model parameter that determines the tissue's sensitivity to fractionation. To determine the optimal fractionation schedule, we can minimize the BED in the organ at risk (OAR) with respect to n and d for a fixed BED

in the tumor. In this paper, we relate to the result published in Ref. 4. In their work, it was shown that the optimal fractionation scheme depends on the α/β-ratios as well as the sparing factor δ for the healthy tissue. (The sparing factor δ is the ratio of the dose received by the tumor and the dose delivered to the OAR.) It was shown that it is optimal to hypofractionate if the α/β-ratio of the OAR is larger than δ times the α/β-ratio of the tumor. Otherwise, hyperfractionation is preferred.

The basic result for BED-based fractionation decisions in Ref. 4 has been extended in different directions. The publications[5–7] consider the case where the OAR is irradiated with an inhomogeneous dose distribution. Other authors have considered extensions of the BED model to incorporate effects from repopulation, the overall treatment time, and incomplete repair.[8,9] In this paper, we consider the extension of BED-based fractionation to the fluence map optimization context. In other words, we consider the simultaneous optimization of the fluence map and the fractionation scheme. In general, this leads to a nonconvex optimization problem for which gradient-based local search methods do not determine the globally optimal solution. Therefore, we consider a stylized model for which we can analyze the structure of the problem and obtain the optimal solution. Despite its simplicity, the model resembles a proton therapy treatment with a single incident beam direction in which a homogeneous dose is to be delivered to the tumor while sparing the healthy tissue in the entrance region of the beam. In particular, we minimize the cumulative BED in the beam entrance region, subject to the constraint that every tumor voxel receives the prescribed BED at the end of treatment. To keep the model tractable, we assume that the treatment consists of two different fluence maps that are delivered in subsequent fractions in an alternating fashion. The model provides insight into the structure of the optimal treatment. It is shown that

- if the α/β-ratio of the tumor is very large, it is optimal to deliver a hyperfractionated treatment in which the dose is evenly distributed between the two fractions and the same treatment plan is delivered.
- if the α/β-ratio of the tumor is small, it is optimal to hypofractionate, i.e., deliver all of the dose in one of the two fractions and zero dose in the subsequent fraction.
- in the intermediate range of α/β values, a new type of treatment regimen emerges in which two different dose distributions are delivered in subsequent fractions.

The latter treatment regimen does not arise when the determination of the fractionation scheme is decoupled from the optimization of the fluence map. It requires the simultaneous optimization of fractionation scheme and dose distribution. The intuitive explanation for this phenomenon is as follows: By varying the dose distribution in the tumor between fractions, we can achieve the same total BED with a lower physical dose. If it is possible to achieve this dose variation in the tumor without varying the dose in the OAR between fractions (which would have an adverse effect), the reduction in physical dose may lead to a net reduction in the BED in the OAR. For proton therapy, this is indeed possible to some degree because the entrance dose of a proton beam remains mostly unchanged between pencil beams that deliver dose to the distal or proximal part of the target, respectively. This idea has been introduced in Refs. 10 and 11.

The remainder of this paper is organized as follows: In Sec. 2, we define the optimization problem to simultaneously optimize fluence maps and fractionation scheme. Section 3 introduces the proton therapy model. The structure of the optimal treatment and its dependence on parameters, in particular the α/β-ratios, is analyzed in Sec. 4. In Sec. 5, we estimate the magnitude of normal tissue sparing that is achievable through nonuniform fractionation schemes. In Sec. 6, we discuss the results.

2. GENERAL PROBLEM FORMULATION

In this section, we formulate the radiotherapy planning problem to simultaneously optimize fluence maps and fractionation schedule. In the classical fluence map optimization problem for photon or proton therapy, we consider an objective function $f(\boldsymbol{d})$ and constraint functions $c_k(\boldsymbol{d})$ which are typically convex functions of the dose distribution $\boldsymbol{d}$. The dose distribution is a linear function of the fluence map $\boldsymbol{x}$. In treatment planning, we seek to solve an optimization problem of the following form:

$$\underset{x}{\text{minimize}} \quad f(\boldsymbol{d}), \tag{2}$$

$$\text{subject to} \quad c_k(\boldsymbol{d}) \leq u_k \quad \forall k, \tag{3}$$

$$d_i = \textstyle\sum_j D_{ij} x_j \quad \forall i, \tag{4}$$

$$x_j \geq 0 \quad \forall j, \tag{5}$$

where u_k are upper bounds for the constraint functions and D_{ij} is the dose-influence matrix. In photon therapy, x_j is the intensity of beamlet j; in proton therapy x_j is the intensity of pencil beam j. In current practice, the same fluence map $\mathbf{x}$ is delivered in every fraction t, yielding the same dose distribution.

We now aim at simultaneously optimizing n possibly distinct fluence maps $\mathbf{x_t}$, where n is the number of fractions. This will be performed using the concept of BED. To that end, we generalize the BED equation in Eq. (1) to the situation in which different doses are delivered in different fractions. The cumulative BED in voxel i over the entire treatment is then given by

$$b_i = \sum_{t=1}^{n} \left[d_{ti} + \left(\frac{\beta}{\alpha}\right)_i d_{ti}^2 \right], \tag{6}$$

where d_{ti} is the physical dose delivered to voxel i in fraction t and $(\beta/\alpha)_i$ is the inverse of the α/β ratio of the tissue that voxel i belongs to. In principle, we can apply the same objective and constraint functions for treatment planning as before, except that we evaluate these functions for the cumulative BED instead of the physical dose. We can thus formulate the simultaneous optimization of fluence maps and fractionation schedule as the following problem:

$$\underset{x}{\text{minimize}} \quad f(\boldsymbol{b}), \tag{7}$$

$$\text{subject to} \quad c_k(\boldsymbol{b}) \leq u_k \quad \forall k, \tag{8}$$

$$b_i = \sum_{t=1}^{n} b_{ti} \quad \forall i, \tag{9}$$

$$b_{ti} = d_{ti} + \left(\frac{\beta}{\alpha}\right)_i d_{ti}^2 \quad \forall i, \forall t, \tag{10}$$

$$d_{ti} = \sum_j D_{ij} x_{tj} \quad \forall i, \forall t, \tag{11}$$

$$x_{tj} \geq 0 \quad \forall j, \forall t. \tag{12}$$

The problem formulation (7)–(12) allows for optimal solutions with distinct dose distributions delivered in different fractions. This is due to the nonlinear, i.e., quadratic dependence of the cumulative BED on the fraction doses. Because of the quadratic term, different total physical doses can lead to the same BED, an effect that can be exploited in this formulation of the problem. In particular, if it is optimal to hypofractionate, fluence maps for a subset of the treatment fractions will be zero at the optimal solution. In that sense, the formulation simultaneously optimizes fractionation scheme and dose distributions.

2.A. Nonconvexity of the problem

Although the problem of simultaneously optimizing for fluence maps and fractionation scheme can be formulated, solving the problem to optimality is inherently difficult because the problem is nonconvex. Even if f and c_k are convex functions of BED, the problem is nonconvex due to the quadratic equality constraints (9) that relate dose and BED. Alternatively, we can consider f and c_k explicitly as a function of the fluence maps $\mathbf{x_t}$. As an example, we can consider a quadratic objective function f that penalizes the deviation of the cumulative BED from a prescribed BED. Since BED is a quadratic function of the intensities x_{tj}, the objective function becomes a fourth-order polynomial in the decision variables—thus representing a generally nonconvex problem. The nonconvexity will become apparent for the concrete example discussed in the remainder of the paper. An approach to address the problem of nonconvexity when solving the problem (7)–(12) for a real patient geometry is outlined in Sec. 6.D.

2.B. A specific IMPT planning problem

In the remainder of the paper, we consider a particular instantiation of the planning problem (7)–(12). The set of constraint functions is obtained by requiring that all tumor voxels receive the prescribed BED b^p at the end of treatment. In the objective function, we minimize the integral BED in all healthy tissues. The optimization problem can be formulated as

$$\underset{x}{\text{minimize}} \quad \sum_{i \notin T} b_i, \tag{13}$$

$$\text{subject to} \quad b_i = b^p \quad \forall i \in T \tag{14}$$

together with the BED and dose defining constraints (9)–(12). Here, T denotes the set of all tumor voxels. This represents an objective function that is quadratic in the beam intensities x_{tj}, has bound constraints on the decision variables x_{tj}, and has equality constraints that are quadratic functions of x_{tj}. Due to the equality constraints, this represents a nonconvex optimization problem. Note that this problem formulation suits the proton therapy model that is introduced in Sec. 3, whereas for a real clinical case, the equality constraints (14) have to be relaxed.

3. A MODEL OF PROTON THERAPY WITH A SINGLE BEAM

Due to the nonconvexity of the treatment planning problem (7)–(12), it is difficult to obtain the optimal solution for a clinical case. We therefore consider a simplified case which we can solve exactly and which provides insight into the structure of the problem. The model mimics a proton therapy treatment with a single incident beam direction. The proton field is modeled via two proton beams with different range. Beam 1 delivers dose primarily to the distal part of the tumor; beam 2 delivers dose to the proximal part of the tumor. The patient is represented by four volumes of interest (voi) as illustrated in Fig. 1. Voi 1 is a normal tissue voxel in the entrance region of the proton beam. Vois 2 and 3 are tumor subvolumes corresponding to the proximal and distal part of the target, respectively. Voi 4 is a normal tissue region distal to the tumor. We assume that the tumor vois are characterized by an α/β-ratio which we denote by $(\alpha/\beta)_T$. In the normal tissue vois 1 and 4, the α/β ratio is assumed to be the same and denoted by $(\alpha/\beta)_N$. This could, of course, be generalized to different α/β-ratios.

3.A. Dose-influence matrix

We define a dose-influence matrix D_{ij} that quantifies the dose contributions of the two proton beams j to the four vois i. For the results presented in this paper, we choose the following values:

$$\begin{pmatrix} D_{11} & D_{21} & D_{31} & D_{41} \\ D_{12} & D_{22} & D_{32} & D_{42} \end{pmatrix} = \begin{pmatrix} 0.3 & 0.5 & 1.0 & 0.1 \\ 0.4 & 1.0 & 0.1 & 0.0 \end{pmatrix}. \tag{15}$$

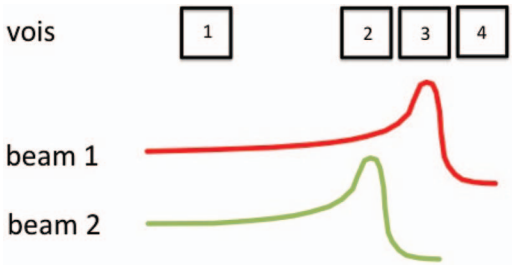

FIG. 1. Stylized model that mimics a proton therapy treatment with a single incident beam direction. The patient is represented by 4 volumes: vois 2 and 3 represent the proximal and distal section of the tumor, whereas 1 and 4 represent normal tissues. The tumor is irradiated by two proton beams. Beam 1 primarily irradiates the distal part of the tumor, whereas beam 2 covers the proximal part.

This geometry mimics the most important features of a proton treatment with a single incident beam direction: (i) The distal beam delivers a significant dose also to the proximal part of the target, in this case half the dose that is delivered to the distal part. (ii) The distal beam also delivers some dose to healthy tissue surrounding the distal part of the tumor, which is modeled by the 10% dose contribution to voi 4. (iii) The proximal beam delivers a slightly higher dose to voi 1 which represents the entrance region.

3.B. Fractionation schemes

We assume that the complete treatment will consist of up to n fractions, where we assume that n is an even number. To keep the problem tractable, we assume that only two fractions are different, i.e., we optimize two distinct fluence maps that are delivered in subsequent fractions in an alternating fashion. Both fluence maps are delivered $n/2$ times over the course of treatment. If both fluence maps are equal, i.e., in all n fractions the same dose distribution is delivered, we refer to this scheme as the hyperfractionated regimen. If one of the fluence maps delivers zero dose, we refer to this scheme as the hypofractionated regimen because all the dose is delivered in $n/2$ fractions.

3.C. Treatment plan optimization problem

We now consider the optimization problem formulated in Eqs. (13) and (14) together with the BED and dose defining constraints (9)–(12). For the model in Fig. 1, we have $t \in \{1, 2\}$, $j \in \{1, 2\}$, and $i \in \{1, 2, 3, 4\}$ and we can write the optimization problem for the stylized model explicitly as

$$\underset{x}{\text{minimize}} \quad b_{11} + b_{21} + b_{14} + b_{24}, \tag{16}$$

$$\text{subject to} \quad b_{1i} + b_{2i} = b^p \quad i \in \{2, 3\}, \tag{17}$$

$$x_{tj} \geq 0 \quad j \in \{1, 2\},\ t \in \{1, 2\}. \tag{18}$$

In total, we have four decision variables x_{ti}. Only two out of the four variables are independent because the remaining two are determined by the two equality constraints (17). For the discussion in this paper, we will consider the fluence map of the first fraction (x_{11}, x_{12}) as independent variables. We want to express the fluence map (x_{21}, x_{22}) of the second fraction as a function of the first fluence map. For that, we note that the first fluence map determines the physical dose d_{1i} and the BED b_{1i} delivered in the first fraction. From the tumor BED constraints, we obtain the BED values b_{22} and b_{23} that are to be delivered to the tumor voxels in the second fraction. From the BED values, we obtain the physical dose distribution d_{22} and d_{23} that is to be delivered in the second fraction. This relation is given by

$$d_{2i} = -\frac{1}{2}\left(\frac{\alpha}{\beta}\right)_i + \sqrt{\frac{1}{4}\left(\frac{\alpha}{\beta}\right)_i^2 + \left(\frac{\alpha}{\beta}\right)_i b_{2i}}, \tag{19}$$

where b_{2i} is a quadratic function of the first fluence map. From the two physical doses d_{22} and d_{23}, we obtain the second fluence map by solving a set of two linear equations given by $d_{2i} = D_{i1}x_{21} + D_{i2}x_{22}$ for $i \in \{2, 3\}$. However, it is due to the square root relation in Eq. (19) that the objective function has a nontrivial, nonconvex shape when considered as a function of the two independent variables (x_{11}, x_{12}) alone.

4. OPTIMAL TREATMENT SCHEDULES

In this section, we perform a detailed analysis of the optimal treatment regimen depending on the α/β-ratios of tumor and normal tissue. We perform this analysis by varying the α/β-ratio for the tumor while choosing a fixed value of $(\alpha/\beta)_N = 3$ for the healthy tissue. We further choose the prescribed cumulative BED over two fractions as $b^p = 4.8$ Gy. This corresponds to a standard fractionated treatment with 2 Gy per fraction assuming $(\alpha/\beta)_T = 10$.

4.A. Hypofractionation regimen

We start the discussion by considering the case where the α/β-ratio in the tumor is in the same range as the α/β-ratio in the normal tissue. Figure 2 shows the objective function (16) as a function of the pencil beam weights (x_{11}, x_{12}) in the first fraction for $(\alpha/\beta)_T = 2$. We discuss the figure in detail:

- The thick solid black lines mark the boundary of the feasible region, i.e., the region of (x_{11}, x_{12}) values for which there is a second fluence map (x_{21}, x_{22}) such that the prescribed tumor BED in both target vois is met.
- The dashed black line marks the treatments for which a homogeneous dose is delivered to the tumor in each fraction, i.e., both tumor vois receive the same dose. For the dose-influence matrix in Eq. (15), this is the case if the weight of the proximal beam is 5/9 of the weight of the distal beam.
- Along the dashed line of homogeneous treatments, we find the classical hyperfractionation scenario, which corresponds to the point $(x_{11}, x_{12}) = (1.36, 0.74)$ that is marked by the dot. Calculating the second fluence map for this point yields $(x_{21}, x_{22}) = (x_{11}, x_{12})$. The hyperfractionation plan is a unique point within the feasible region: It represents a stationary point of the objective function, in this case a maximum. This means that, for

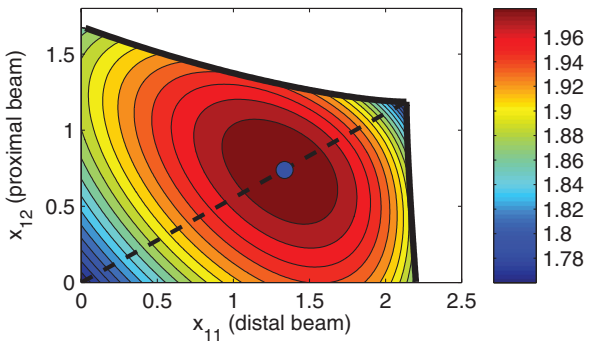

FIG. 2. Integral BED in the normal tissue for $(\alpha/\beta)_T = 2$ and $(\alpha/\beta)_N = 3$. The optimal solution corresponds to a hypofractionation regimen where both beam weights are zero in one of the fractions.

this set of parameters, hyperfractionation leads to the highest normal tissue BED and is the least favorable treatment.

- In the corners of the feasible region that are connected by the dashed line, we find the hypofractionation scheme. If $(x_{11}, x_{12}) = (2.14, 1.19)$, all dose is delivered using the first fluence map, (x_{21}, x_{22}) evaluates to zero. Conversely, at $(x_{11}, x_{12}) = (0, 0)$, all dose is delivered by the second fluence map. The objective function values at these two solutions are equal. In this case, the hypofractionation plan yields the lowest integral normal tissue BED and is thus the optimal treatment. The cumulative BED in the two normal tissue vois decreases to 1.76 compared to 2.00 for the hyperfractionation plan.
- All plans that are not along the dashed line correspond to treatments in which an inhomogeneous dose is delivered to the tumor in each fraction. In the corner of the feasible region, at $(x_{11}, x_{12}) = (2.23, 0)$ we find a treatment in which only the distal beam is used in the first fraction, and only the proximal beam in the second fraction. The point $(x_{11}, x_{12}) = (0, 1.8)$ is equivalent except that the fractions are interchanged. These points correspond to local minima, but not the global minimum.
- In our problem formulation, the BED has no explicit or implicit time dependence. As a consequence, we can interchange fraction one and two without changing the objective function value. In Fig. 2, this becomes manifest in the observation that every point in the feasible region has a corresponding point that defines the fluence map of the second fraction. Loosely speaking, this point is located diagonally across from the point under consideration.

In summary, for $(\alpha/\beta)_T = 2$ and $(\alpha/\beta)_N = 3$ we observe that hypofractionation is the optimal treatment decision, whereas hyperfractionation leads to the highest normal tissue BED. This is in agreement with the expected result for very low tumor α/β.

4.B. Hyperfractionation regimen

We now turn to the other extreme case of very large α/β-values in the tumor. We consider the case $(\alpha/\beta)_T \to \infty$ for which the quadratic term in the BED equation vanishes. In this case, the BED in the tumor equals the physical dose, and the tumor is insensitive to fractionation. Figure 3 shows the objective function (16) as a function of the pencil beam weights in the first fraction for $(\alpha/\beta)_T \to \infty$. We make several observations:

- The objective function has a unique minimum which occurs at the pencil beam weights $(x_{11}, x_{12}) = (2.27, 1.26)$ as marked by the dot. Calculating the fluence map for the second fraction yields $(x_{21}, x_{22}) = (x_{11}, x_{12})$ such that this solution corresponds to a hyperfractionation plan in which the same, homogeneous dose is delivered to the tumor in both fractions. This result is intuitive: For the tumor, only the total physical dose is important, whereas for the normal tissue voxels it is optimal to deliver equal doses in both fractions. For the OAR voxel distal to the tumor, this is only possible if the weight of the distal pencil beam is the same in both fractions.
- Hypofractionation is the worst choice for large $(\alpha/\beta)_T$ values. The integral BED in the normal tissue increases from 3.80 for hyperfractionation to 4.78 for hypofractionation.
- We observe that the minimum is shallow. At $(x_{11}, x_{12}) = (3.79, 0)$, we deliver only the distal beam (at higher intensity) in the first fraction. In the second fraction, the proximal beam is delivered together with the remaining intensity of the distal beam ($(x_{21}, x_{22}) = (0.76, 2.53)$). This treatment yields an integral BED of 3.82 in the normal tissue — only a slight increase compared to the optimum. This is because this type of treatment delivers a similar dose to the proximal normal tissue voi, which yields the largest contribution to the objective function. The fact that hyperfractionation is a unique minimum is due to the distal normal tissue voi. In fact, if the distal normal tissue voi is neglected in the objective function, there is no unique optimal solution, i.e., many treatments yield the same normal tissue BED.

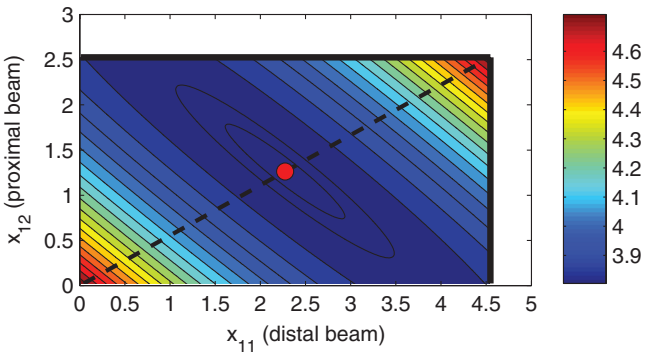

FIG. 3. Integral BED in the normal tissue for $(\alpha/\beta)_T \to \infty$ and $(\alpha/\beta)_N = 3$. For these parameter values, the normal tissue is sensitive to fractionation, whereas the effect in the tumor only depends on the physical dose. In this case, hyperfractionation with equal dose distributions in all fractions is optimal.

4.C. The emergence of inhomogeneous fractional doses (IFD)

We now consider $(\alpha/\beta)_T = 10$. The objective function is shown is shown in Fig. 4. We first observe that the hypofractionation regimen is unfavorable, which is expected because the tumor $(\alpha/\beta)_T$ is larger than $(\alpha/\beta)_N$ times the effective sparing factor for the normal tissue. In fact, the hyperfractionated treatment is preferable over hypofractionation. However, we observe that hyperfractionation is now a saddle point of the objective function. The global optima are given by $(x_{11}, x_{12}) = (3.4, 0)$ and $(x_{11}, x_{12}) = (0, 2.28)$. These solutions correspond to treatments in which different dose distributions are delivered in both fractions. In the remainder of this paper, we refer to this type of treatment as inhomogeneous fractional doses (IFD). The solution $(x_{11}, x_{12}) = (3.4, 0)$ means that in the first fraction only the distal pencil beam

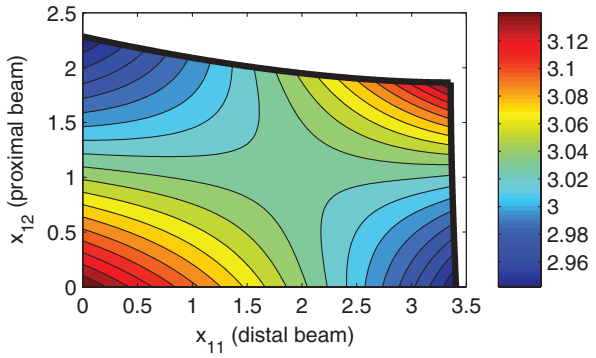

FIG. 4. Integral BED in the normal tissue for $(\alpha/\beta)_T = 10$ and $(\alpha/\beta)_N = 3$. The optimal solution occurs for $(x_{11}, x_{12}) = (3.4, 0)$ and $(x_{21}, x_{22}) = (0, 2.28)$. This corresponds to an IFD treatment in which the distal portion of the tumor is irradiated in one fraction and the proximal part in the subsequent fraction.

is used. Calculating the fluence map for the second fraction yields $(x_{21}, x_{22}) = (0, 2.28)$, which means that only the proximal pencil beam is used in the second fraction. Since there is no time dependence of the α/β-ratios, both fractions can be interchanged to yield the same BED in the normal tissue.

4.D. Transitions

We now discuss the critical values of $(\alpha/\beta)_T$ at which transitions between treatment regimens occur or at which the objective function qualitatively changes.

4.D.1. Transition from hyperfractionation to IFD

We have discussed above that for very large $(\alpha/\beta)_T$, hyperfractionation is the optimal treatment regimen. The transition to inhomogeneous fractional doses occurs when the hyperfractionation treatment turns from a local minimum into a saddle point. This occurs for $(\alpha/\beta)_T = 89$ as shown in Fig. 5. For this parameter value, the optimal treatment regimen is degenerate. For smaller values of $(\alpha/\beta)_T$, IFD type treatments start to dominate over hyperfractionation (as in Fig. 4). It is noted that the transition from hyperfractionation

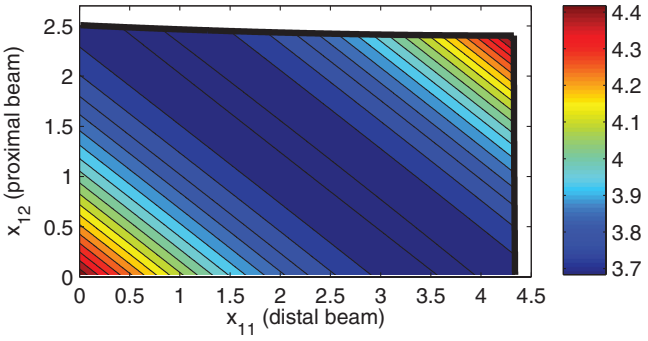

FIG. 5. Integral BED in the normal tissue for $(\alpha/\beta)_T = 89$ and $(\alpha/\beta)_N = 3$. For these parameter values, hyperfractionation and IFD type treatments lead to the same normal tissue BED. The hyperfractionation point turns from a minimum into a saddle point.

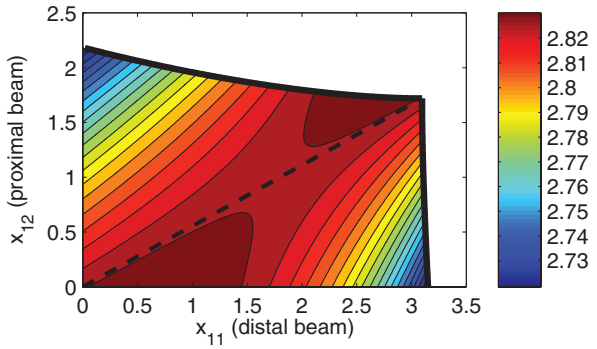

FIG. 6. Integral BED in the normal tissue for $(\alpha/\beta)_T = 6.97$ and $(\alpha/\beta)_N = 3$. For these parameter values, hyper- and hypofractionation are equal. The optimal solution is, however, an IFD treatment.

to IFD coincides with a qualitative change in the objective function, i.e., a transition of the hyperfractionation point from a minimum to a saddle point.

4.D.2. The homogeneous transition from hyper- to hypofractionation

We now consider all treatments in which a homogeneous dose is delivered to the tumor in both fractions. Using the results previously published by Mizuta[4] and the generalization to inhomogeneous OAR dose distributions,[6] we can calculate the tumor α/β-ratio at which the transition from hyper- to hypofractionation for homogeneous dose distributions occurs. It has been shown that this transition occurs if $(\alpha/\beta)_N = \bar{\delta}(\alpha/\beta)_T$, where

$$\bar{\delta} = \frac{\sum_i \delta_i^2}{\sum_i \delta_i} \tag{20}$$

is an effective sparing factor for an inhomogeneously irradiated normal tissue. The summation is carried out over all voxels i and δ_i is the sparing factor in voxel i, i.e., the dose received by the voxel divided by the tumor dose. For the dose-influence matrix in Eq. (15), the effective sparing factor evaluates to $\bar{\delta} = (\delta_1^2 + \delta_4^2)/(\delta_1 + \delta_4) = 0.43$. Consequently, hyper- and hypofractionation become equal for $(\alpha/\beta)_T = (\alpha/\beta)_T/\bar{\delta} = 6.97$. Figure 6 shows the objective function for this value. It is apparent that all homogeneous dose treatments along the dashed line lead to equal integral normal tissue BED. (Note that the BED in individual vois can change.) We also observe that the objective function landscape, for the problem of simultaneously optimizing both fluence maps, does not qualitatively change at the homogeneous transition point, i.e., the hyperfractionation plan is a saddle point. In particular, we observe that for a range of $(\alpha/\beta)_T$ values above and below the homogeneous transition point, IFD type treatments are optimal.

4.D.3. Hyperfractionation becomes the least favorable treatment

For $(\alpha/\beta)_T = 6.68$, the hyperfractionation treatment turns from a saddle point into a local maximum as shown in Fig. 7.

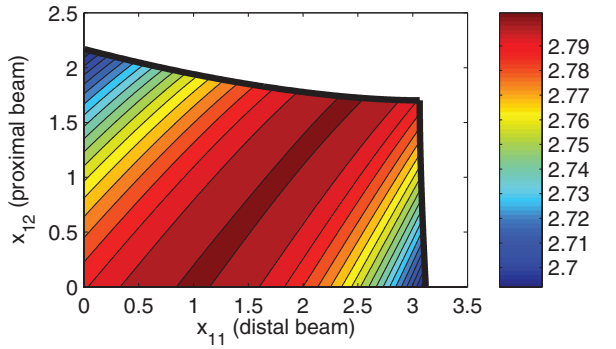

FIG. 7. Integral BED in the normal tissue for $(\alpha/\beta)_T = 6.68$ and $(\alpha/\beta)_N = 3$. For these parameter values, hyperfractionation becomes the least favorable treatment regimen. The optimal solution is an IFD type treatment.

For smaller values of $(\alpha/\beta)_T$, all treatments lead to lower integral BED than hyperfractionation. However, even though the objective function qualitatively changes, this value of $(\alpha/\beta)_T$ does not correspond to a qualitative change in the optimal treatment regimen—unlike the transition from a minimum to a saddle point. In a range of $(\alpha/\beta)_T$ values above and below 6.68, IFD treatments are optimal.

4.D.4. The transition from IFD to hypofractionation

The transition between IFD treatments and hypofractionation occurs when all local minima in the four corners of the feasible region have equal objective values. This occurs at $(\alpha/\beta)_T = 4.4$ as shown in Fig. 8. For $(\alpha/\beta)_T$ values above and below 4.4, hyperfractionation is a maximum of the objective function. Hence the transition from IFD to hypofractionation does not coincide with a qualitative change of the objective function. In addition, we note that the transition is discontinuous in the sense that the optimal IFD solution and hypofractionation are in distinct regions of the search space. This is in contrast to the transition from hyperfractionation to IFD, where the optimal solution is degenerate and a continuum of optimal plans between hyperfractionation and IFD treatments exists.

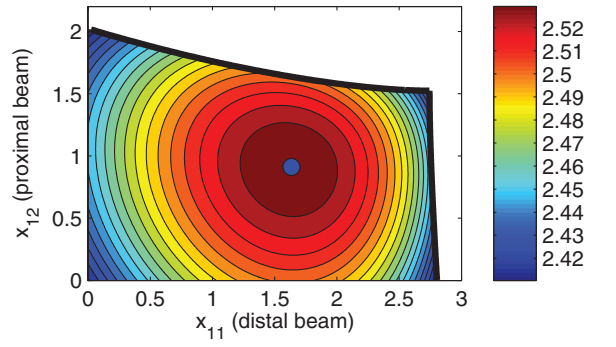

FIG. 8. Integral BED in the normal tissue for $(\alpha/\beta)_T = 4.4$ and $(\alpha/\beta)_N = 3$. For these parameter values, hypofractionation and the optimal IFD type treatment lead to the same normal tissue BED.

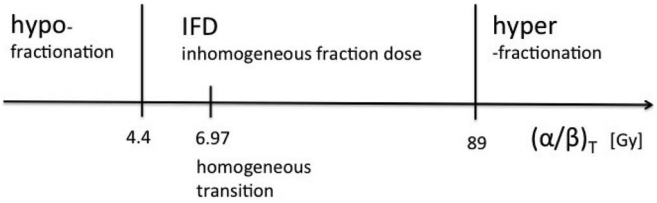

FIG. 9. Optimal fractionation schemes depending on $(\alpha/\beta)_T$ for $(\alpha/\beta)_N = 3$, summarizing the results of Sec. 4. Around the homogeneous transition from hyper- to hypofractionation at $(\alpha/\beta)_T = 6.97$, a nonuniform fractionation scheme emerges in which it is optimal to deliver two distinct fluence maps in subsequent fractions.

4.E. Summary

We consider the simultaneous optimization of two fluence maps for a proton therapy treatment with a single incident beam direction. This can be considered as a generalization of the optimal fractionation problem based on the BED model to the fluence map optimization context. It is demonstrated that, depending on the α/β ratios in the tumor and the normal tissue, three types of fractionation schemes arise. This is schematically illustrated in Fig. 9. If the α/β-ratio of the tumor is very large, it is optimal to deliver a hyperfractionated treatment in which the dose is evenly distributed between the two fractions and the same treatment plan is delivered. On the contrary, if the α/β-ratio of the tumor is small, it is optimal to hypofractionate, i.e., deliver all of the dose in one of the two fractions and zero dose in the other fraction. In the intermediate range of α/β values, a new type of treatment regimen emerges in which two different dose distributions are delivered in subsequent fractions. We refer to this treatment regimen as IFD.

5. THE POTENTIAL BENEFIT OF IFD TREATMENTS

In this paragraph, we discuss the potential benefit of IFD treatments by quantifying the BED reduction in normal tissues. The benefit of IFD treatments depends on a number of factors, including

- the α/β-ratios in the tumor and normal tissues,
- the average prescribed tumor BED per fraction (i.e., the parameter b^p),
- the dose distribution in the normal tissue,
- the planning goals (i.e., the question whether integral BED is to be minimized, reduction of skin dose is the primary goal, or a serial structure close to the tumor is dose limiting),
- the patient geometry and the incident beam directions.

5.A. The benefit for 2 Gy per fraction and $(\alpha/\beta)_T = 10$

We first consider the benefit of IFD treatments for typical parameters, i.e., $(\alpha/\beta)_T = 10$ and a physical dose of 2 Gy per fraction in the hyperfractionation scenario, which corresponds to a prescribed BED of $b^p = 4.8$ over two fractions.

It is instructive to first consider the hypothetical maximum benefit that was achievable through IFD if we could vary the tumor dose arbitrarily without changing the dose in the normal tissue. Assuming one could deliver the entire BED to the distal tumor voi in one fraction and the entire BED to the proximal part in the second fraction. Then, the physical dose to each tumor voxel could be reduced to 3.54 Gy compared to 4 Gy, which corresponds to a reduction of 11.5%. Depending on the value of $(\alpha/\beta)_N$ and the sparing factor, this leads to a similar reduction of BED in the normal tissue. Clearly, this only represents an upper bound for the benefit of IFD.

The model analyzed in this paper provides an estimate about the actual BED reduction in normal tissue that is achievable through IFD treatments with realistic proton beams. We consider the parameters $(\alpha/\beta)_T = 10$ and $(\alpha/\beta)_N = 3$ used in Fig. 4. For this set of parameters, the difference in normal tissue BED between the hyperfractionation plan (3.035 Gy) and the optimal IFD plan (2.942 Gy) is 3% of the hyperfractionated plan. This demonstrates that the hypothetical maximum benefit of 11.5% described above is not achievable with realistic proton beams because we cannot arbitrarily redistribute dose in the tumor without changing the dose distribution in the normal tissue.

Considering that the benefit of IFD may be further reduced for realistic patient geometries and planning goals (see Sec 5.D.), we conclude that the benefit of alternating two distinct dose distributions will probably not be clinically significant for tumors treated with standard fractionation at 2 Gy per fraction.

5.B. Dependence on the α/β ratios

In the model, hyper- and hypofractionation become equal for $(\alpha/\beta)_T = 6.97$. In this case, the best IFD treatment (normal tissue BED of 2.72 Gy) yields a 3.9% improvement over hyperfractionation (BED of 2.83 Gy) as seen in Fig. 6. This represents a larger benefit compared to $(\alpha/\beta)_T = 10$. For smaller values of $(\alpha/\beta)_T$, the benefit of IFD over hyperfractionation increases further, however, in this situation hypofractionation starts to dominate over hyperfractionation. Thus, for a fair assessment of the benefit of IFD over any uniform fractionation scheme, one has to compare IFD to hypofractionation. The benefit of IFD becomes zero at the transitions point to hypofractionation at $(\alpha/\beta)_T = 4.4$ (Fig. 8) and at the transition to hyperfractionation $(\alpha/\beta)_T = 89$.

5.C. Dependence on the dose per fraction

The expected benefit of IFD treatments increases with higher dose per fraction. In our model, this is controlled by the parameter b^p, the prescribed BED over two fractions. In Sec. 4, we use $b^p = 4.8$ Gy, which corresponds to a dose of 2 Gy per fraction assuming $(\alpha/\beta)_T = 10$. If we assume a total of 30 fractions, this corresponds to a standard fractionated treatment with a total BED of 72 Gy. If we increase the prescribed BED per fraction, the benefit of IFD over hyperfractionation increases. As an example, we look at the case $b^p = 36$ Gy, which corresponds to 4 fractions at 9.31 Gy in the hyperfractionation scenario[12] and 2 fractions at 14.62 Gy in the hypofractionation scenario. Plotting the normal tissue BED for $(\alpha/\beta)_T = 10$ and $(\alpha/\beta)_N = 3$ yields a result that is qualitatively the same as the one shown in Fig. 4. However, the difference of the optimal IFD treatment over hyperfractionation increases to 7.6%. The cumulative normal tissue BED over 2 fractions decreases from 25.67 Gy for the hyperfractionated treatment to 23.72 Gy for the IFD treatment. For the case $b^p = 72$ Gy, which corresponds to 2 fractions at 14.62 Gy in the hyperfractionation scenario and 1 fraction at 22.29 Gy in the hypofractionation scenario, the benefit of IFD over hyperfractionation increases to 8.9%.

5.D. Dependence on planning goals and dose distribution

The benefit of IFD depends on the dose distribution in the normal tissue and on planning goals. The results presented in Sec. 4 are dominated by the BED in the proximal normal tissue voi. The model mimics the situation in which we aim at minimizing BED in the low dose region or the skin. The small dose contribution to a distal voi has a small effect, which mostly becomes visible in the limit of large $(\alpha/\beta)_T$ values where it causes hyperfractionation to be optimal. However, realistic proton beams, especially if margins are added to account for range and setup uncertainty, deliver dose to normal tissue close to the tumor. If a critical organ is located near the tumor, reducing the normal tissue BED close to the tumor may be a primary planning goal. In our idealized model, we can mimic this situation via a modification of the dose-influence matrix: We replace the dose contribution D_{41} to a value of

$$D_{41} = 1.0, \tag{21}$$

so that the distal normal tissue voi receives the same dose as the distal tumor voi when the distal beam is used. This mimics the clinical use of a distal safety margin in proton therapy. In this numerical example, the benefit of IFD almost vanishes. In particular, for $(\alpha/\beta)_T = 10$, hyperfractionation is optimal. This is because the BED in the distal voi greatly increases if the distal beam has different weights in the two fractions. Around the homogeneous transition point at $(\alpha/\beta)_T = 3.79$, where hyper- and hypofractionation are equal, there is a small residual benefit for IFD treatments that originates from the contribution of the proximal voi. This is shown in Fig. 10. However, the BED reduction is only 0.35% of the BED for the hyperfractionation plan. Figure 10 also shows that the objective function landscape is very different compared to Fig. 6. An IFD treatment at the corner of the feasible region, i.e., each fraction uses either the distal or the proximal beam but not both, is the least favorable treatment. In contrast, in Fig. 6 where the objective function is dominated by the proximal voi, such treatments are optimal.

The two dose-influence matrices in Eqs. (15) and (21) can be considered as two extreme cases. In the original dose-influence matrix (15), the planning objective for the normal

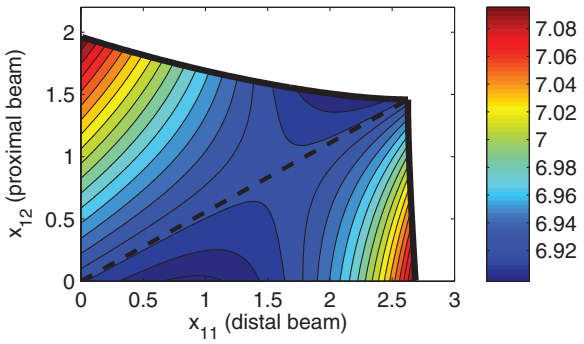

FIG. 10. Integral BED in the normal tissue for $(\alpha/\beta)_T = 3.79$, $(\alpha/\beta)_N = 3$, and the dose-influence matrix modification in Eq. (21). For these parameter values, hyper- and hypofractionation are equal. The IFD treatment at $(x_{11}, x_{12}) = (0.9, 0)$ yields a small benefit over uniform treatments.

tissue is dominated by low doses in the beam path, which leads to the benefit for IFD. In contrast, for the modified dose-influence matrix (21), the normal tissue objective is dominated by the normal tissue adjacent to the target treated to a high dose. In particular, in this example, it is not possible to alter the tumor dose between fractions without varying the OAR dose by a similar amount, which eliminates the benefit of IFD and illustrates that:

- to maintain a benefit of IFD, reducing the skin BED or the mean BED in the low dose region in the beam entrance path has to be a significant planning goal.
- An OAR near (or within) the target receiving high doses will typically work against the benefit of IFD. In this situation, varying fractional doses at the edge of the target (leading to dose variations and BED increases in the OAR) become unfavorable.

Realistically, there is a tradeoff between reducing integral BED in the entrance region, and increasing the BED in the high dose region within and adjacent to the target volume. The benefit of IFD will therefore depend on the geometry of tumor and OARs as well as the planning goals related to the normal tissues.

- In our model, which minimizes integral BED to normal tissues, the benefit of IFD will depend on the conformity of the dose distribution, i.e., the number of voxels in the entrance region that benefit from IFD has to be large compared to the number of voxels near or within the target.
- If multiple objectives for different OARs conflict, the benefit of IFD will depend on their relative importance.
- Even though OARs adjacent to the target volume tend to reduce the benefit of IFD, the benefit of IFD is not per se neutralized. This situation may limit dose variations between fractions in the part of the target that is located near the OAR. However, if the target volume is large enough, dose variations may occur in the remaining regions of the target volume, and maintain a benefit for IFD.

5.E. Allowing all fractions to be different

In this work, we allowed only two fluence maps to be distinct so that each fluence map is delivered $n/2$ times in a treatment with n fractions in total. Allowing all n fluence maps to be distinct, i.e., a different dose distribution in each fraction, will increase the benefit of IFD treatment plans.

6. DISCUSSION

6.A. Interpretation

The benefit from IFD treatments arises from the fact that we can alter the dose in parts of the tumor from fraction to fraction while varying the dose in normal tissue to a lesser degree. This can be interpreted as hypofractionating subvolumes of the tumor while staying close to standard fractionation in the normal tissue. For proton beams, and also light ion beams, this is possible to some degree because the entrance dose remains mostly the same if the range of the beam is changed. In a treatment geometry with a single incident beam direction, this allows us to irradiate the distal part of the tumor primarily in one fraction, and the proximal part in the subsequent fraction without increasing the BED in the entrance region of the beam.

6.B. Concerns

6.B.1. Susceptibility against uncertainty

IFD type treatments boost different subregions of the tumor in different fractions. This requires dose gradients within the target volume, which potentially make treatment plans more susceptible to setup errors and range uncertainty. This generally represents a concern regarding IFD, but may be acceptable for tumors treated with stereotactic techniques involving accurate immobilization and patient positioning. However, motion and uncertainty may prevent the clinical applicability of IFD to some sites (e.g., hypofractionated lung and liver tumors), which may otherwise have the potential to benefit from IFD.

6.B.2. Validity of the BED model

Our treatment plan optimization model is based on the generalized BED equation (6). In current clinical practice, most patients are treated with the same dose distribution in every fraction, which in many cases is homogeneous in the target. Thus, the clinical validation of the BED model is based on uniform fractionation schemes. Equation (6) represents a generalization of the BED model to nonuniform fractionation schemes and inhomogeneous target dose distributions. This represents a plausible working hypothesis, however its validity is not proven.

6.C. The potential of IFD for clinical tumor sites

In this paragraph, we comment on the tumor sites that potentially benefit from IFD. Summarizing the findings of this

paper, we can state that the tumors with the largest potential to benefit from IFD fulfill the following criteria:

1. The tumor is treated to a relatively large dose per fraction, which increases the advantage of IFD as discussed in Sec. 5.C.
2. IFD treatments can be delivered accurately so that the dose of individual fractions adds up to the prescribed tumor BED, i.e., patient setup and immobilization should be accurate, range uncertainties have to be small.
3. Reducing BED to the skin or the beam entrance region is a planning objective. The volume of normal tissue near or within the target, which is affected by dose variations between fractions, should be small.

To establish a benefit for IFD, these criteria have to be met simultaneously. To assess the clinical potential of IFD, further research and site specific studies are needed, which are outside the scope of this proof-of-concept paper. However, the above criteria can be used to guide the search for a clinical application.

6.C.1. Brain and paraspinal tumors

Criteria 1 and 2 suggest a subset of paraspinal tumors and brain lesions, which are currently treated with stereotactic body radiation therapy (SBRT) or stereotactic radiosurgery (SRS), as candidates for IFD. To what extent criterion 3 is fulfilled further depends on the lesion to be treated, the location and shape of target and OARs, and the planning objectives for additional OARs.

6.C.2. Lung and liver tumors

Lung and liver tumors are two sites for which hypofractionation is currently applied in clinical practice and criterion 1 is fulfilled for a subset of these treatments. In addition, we are interested in sparing healthy lung or liver tissue in the entrance region so that also criterion 3 is fulfilled. However, these tumors are affected by intra- and interfractional anatomy variations. Therefore, degradation of IFD dose distributions due to range uncertainty and motion is a substantial concern.

6.D. Addressing the problem of nonconvexity

It has been pointed out in Sec. 2 that treatment planning based on the BED model leads to nonconvex optimization problems. This has been demonstrated for the concrete example in Sec. 4. Therefore, gradient-based methods will converge to local optima. One approach to address this problem in real patient geometries consists in choosing adequate initializations for the pencil beam weights. This can, for example, be performed according to the following procedure: (1) in a first step, a single treatment plan is optimized which delivers the full dose in one fraction; (2) in the second step, the plan is split into two fractions with equal pencil beam weights; (3) in the last step, the pencil beam weights are redistributed such that the weight of distal spots is increased in fraction one and decreased in fraction two, whereas the proximal weights are decreased in fraction one and increased in fraction two. Based on this initialization of spot weights, a gradient-based method can be applied to find a local optimum to the full problem (7)–(12).

6.E. Further remarks

It has previously been demonstrated that time dependencies in tumor growth and radiation response, such as accelerated repopulation and incomplete repair, may give rise to nonuniform fractionation schemes.[8,9] In this paper, we consider the standard BED model. It is therefore interesting to note that the simultaneous optimization of fractionation schemes leads to nonuniform fractionation schemes that deliver distinct dose distributions in different fractions—even in the absence of any time dependencies in the BED model.

7. CONCLUSIONS

In this paper, we consider the simultaneous optimization of fractionation schemes and fluence maps for radiation therapy planning. This is achieved by formulating the treatment plan optimization problem based on cumulative biologically equivalent dose. An idealized model has been studied that provides insight into the structure of the solution. The model mimics a proton therapy treatment with a single incident beam direction.

It is shown that the combined optimization of fractionation schemes and fluence maps give rise to new treatment schemes in which it is optimal to deliver distinct dose distributions in different fractions. The intuitive explanation for this effect is that, to some degree, the dose distribution in the tumor can be varied, while the dose distribution in the normal tissue remains mostly constant. For proton therapy, this is the case because the dose in the beam entrance region depends only slightly on the range of the proton beam.

Although the projected benefits are likely to be small, the approach bears the potential to improve the therapeutic ratio, in particular, for tumors treated with stereotactic techniques to high doses per fraction. Further work is necessary to fully characterize the potential of nonuniform spatially inhomogeneous fractionation schemes for realistic patient geometries. For that purpose, optimization methods to address the nonconvexity of the BED-based treatment planning problem need to be further developed.

ACKNOWLEDGMENTS

The project was supported by the Federal Share of program income earned by Massachusetts General Hospital on C06 CA059267, Proton Therapy Research and Treatment Center.

[a]Electronic mail: junkelbach@partners.org

[1]J. F. Fowler, "The linear-quadratic formula and progress in fractionated radiotherapy," Br. J. Radiol. **62**(740), 679–694 (1989).

[2]The physical dose distribution is typically determined first. The fractionation scheme is either fixed, or is decided upon based on the given physical dose distribution. For example, the patient's eligibility for hypofractionation may be decided upon based on the amount of normal tissue sparing.
[3]J. F. Fowler, "21 years of biologically effective dose," Br. J. Radiol. **83**(991), 554–568 (2010).
[4]M. Mizuta, S. Takao, H. Date, N. Kishimoto, K. L. Sutherland, R. Onimaru, and H. Shirato, "A mathematical study to select fractionation regimen based on physical dose distribution and the linear-quadratic model," Int. J. Radiat. Oncol., Biol., Phys. **84**(3), 829–833 (2012).
[5]H. Keller, G. Meier, A. Hope, and M. Davison, "Fractionation schedule optimization for lung cancer treatments using radiobiological and dose distribution characteristics," Med. Phys. **39**(6), 3811 (2012).
[6]J. Unkelbach, D. Craft, E. Salari, J. Ramakrishnan, and T. Bortfeld, "The dependence of optimal fractionation schemes on the spatial dose distribution," Phys. Med. Biol. **58**(1), 159–167 (2013).
[7]H. A. Gay, J. Y. Jin, A. J. Chang, and R. K. Ten Haken, "Utility of normal tissue-to-tumor a/b ratio when evaluating isodoses of isoeffective radiation therapy treatment plans," Int. J. Radiat. Oncol., Biol., Phys. **85**(1), e81–e87 (2013).
[8]A. Bertuzzi, C. Bruni, F. Papa, and C. Sinisgalli, "Optimal solution for a cancer radiotherapy problem," J. Math. Biol. **66**(1–2), 311–49 (2013).
[9]Y. Yang and L. Xing, "Optimization of radiotherapy dose-time fractionation with consideration of tumor specific biology," Med. Phys. **32**(12), 2567–2579 (2005).
[10]M. Steneker, A. Trofimov, T. Hong, and M. Engelsman, "Isotoxic dose escalation by increasing tumor dose variance," in *Proceedings of the 16th International Conference on the Use of Computers in Radiation Therapy*, Amsterdam, The Netherlands, *2010*.
[11]C. Zeng, D. Giantsoudi, C. Grassberger, S. Goldberg, A. Niemierko, H. Paganetti, J. A. Efstathiou, and A. Trofimov, "Maximizing the biological effect of proton dose delivered with scanned beams via inhomogeneous daily dose distributions," Med. Phys. **40**(5), 051708 (10pp.) (2013).
[12]We refer to this as hyperfractionation to stay consistent with the terminology in the previous sections. Realistically, a treatment with four fractions is of course not considered hyperfractionated.